Superconductivity in intercalated group-IV honeycomb structures

José A. Flores-Livas and Antonio Sanna
Max-Planck Institut für Microstrukture Physics, Weinberg 2, 06120 Halle, Germany
(Received 9 October 2014; revised manuscript received 9 December 2014; published 9 February 2015)

We present a theoretical investigation on the electron-phonon superconductivity of honeycomb MX_2 layered structures where X is one element of group IV (C, Si, or Ge) and M is an alkali or an alkaline-earth metal. Among the studied compositions we predict a T_C of 7 K in $RbGe_2$, 9 K in $RbSi_2$, and 11 K in SrC_2. All these compounds feature a strongly anisotropic superconducting gap. Our results show that despite the different doping levels and structural properties, the three families of materials fall into a similar description of their superconducting behavior. This allows us to estimate an upper critical temperature of about 20 K for the class of intercalated group-IV structures, including intercalated graphite and doped graphene.

DOI: 10.1103/PhysRevB.91.054508 PACS number(s): 74.70.Wz, 71.20.Tx, 74.20.Pq, 74.25.Jb

Lately, a large research effort has been focused on atomic thin-layered materials and their properties [1–3]. This was triggered by the creation of graphene from graphite [4] and motivated by the belief in many potential applications since thin systems can be significantly modified in their electronic properties simply by acting on parameters as stacking, chemical, and physical doping [5,6]. In fact this versatility is an extraordinary playground for searching for new superconductors (SCs) [7]. Many (low-temperature) SCs are already known in the class of graphite intercalated compounds (GICs) [8–12], graphene itself has been predicted to superconduct with a critical temperature (T_C) of 18 K upon Li doping [13].

Among all possible compounds, those chemically and structurally closer to graphite are the honeycomb lattices of silicon [14–17] and germanium [18,19] for which superconductivity upon intercalation was also reported [14,20–24]. Hence GICs and doped graphene are not unique systems, having Si and Ge counterparts, and can be seen as members of a generalized family of group-IV intercalated honeycomb lattices (gIV-ICs).

So far the highest T_C reported on gIV-ICs is 11.5 K in CaC_6 [11,12]. This system is also the most studied among the family, and its superconducting properties are rather well understood [6,25–28]. It is particularly clear that an important role is played by the existence at the Fermi level of two-dimensional (2D) electronlike bands as well as antibonding C-π states. It is also known that a sufficiently large intercalation is therefore a necessary condition to obtain high critical temperatures. But what is the highest conceivable T_C in an intercalated graphitelike system? Could Si and Ge isomorphs be better candidates than GICs? We will address these questions by focusing our investigation on the high doping limit with one intercalating atom per two honeycomb atoms. We will indicate this family of compounds as MX_2 where M stands for a metal of the I and II columns of the Periodic Table and X is carbon, silicon, or germanium. This composition is known to occur [23] in several silicides [15,21,22] and germanides [18,19,24].

We will show by means of theoretical *ab initio* methods, that finding high-temperature superconductivity in these families is a false hope. On the other hand breaking the record critical temperature of CaC_6 is likely to be possible.

All systems are structurally relaxed within Kohn-Sham density-functional theory (DFT) [29].

Upon relaxation [30] all carbon compounds, apart from CaC_2, converged to the AlB_2 crystal structure (space group $P6/mmm$, number 191), whereas all silicides and germanides as well as CaC_2 converged to the $EuGe_2$ crystal structure (space group $P\bar{3}m1$, number 164). In both, M occupies the $1a$ Wyckoff position (0,0,0), and X occupies the $2d$ positions $(1/3,2/3,z)$ and $(2/3,1/3,-z)$. In the AlB_2 structural prototype the parameter z is fixed at $1/2$, whereas in the $EuGe_2$ structure it is related to a buckling (β) of the honeycomb lattice: $\beta = (|z - 1/2|c)$. The $EuGe_2$ structural prototype and the values of β are shown in Fig. 1. This figure shows clearly that intercalating lighter ions (Li, Be, and Na) induce high-buckled honeycomb plans, whereas heavier ions (Rb, Cs, and Ba) tend to induce low-buckled plans. CaC_2 deviates from the general trend; this structure has a mixture of sp^2-sp^3 (75%–25%, respectively) bonding, and therefore at ambient pressure it presents a finite buckling (energetically more favorable than in a flat AlB_2 structure). In this respect, it recently has been predicted by Li and co-workers [31] that the flat-layered phase could be stabilized at high pressures.

As many of the compounds discussed in this paper are not experimentally known, in order to assert their potential synthesis, we calculated their thermodynamic stability, which is derived from the total DFT energy of the system (MX_2) and of its elemental ground-state solid (see Supplemental Material [30] for details). This analysis leads to the conclusion that all graphite compounds in the MX_2-layered phase are unstable towards this elemental decomposition, whereas most of silicides and germanides are stable towards decomposition. Nevertheless, since a positive formation energy does not completely exclude these materials from their possible synthesis, we will also investigate their dynamical stability (phonons).

For all systems under investigation we computed phonons, and only for those systems dynamically stable, the electron-phonon coupling was calculated by means of density-functional perturbation theory [32]. We found most of the intercalated carbon compounds to be dynamically unstable with the only exception of Sr and Ca intercalation. This suggests that the 1 to 2 intercalation is too large for this family and is evidenced experimentally by the reported challenging synthesis of LiC_2 [8], that turns out to be metastable, partially losing its Li content and converting in LiC_6 [9,10]. On the other hand, with the exception of light-ion intercalants, most of the disilicides and digermanides are dynamically stable.

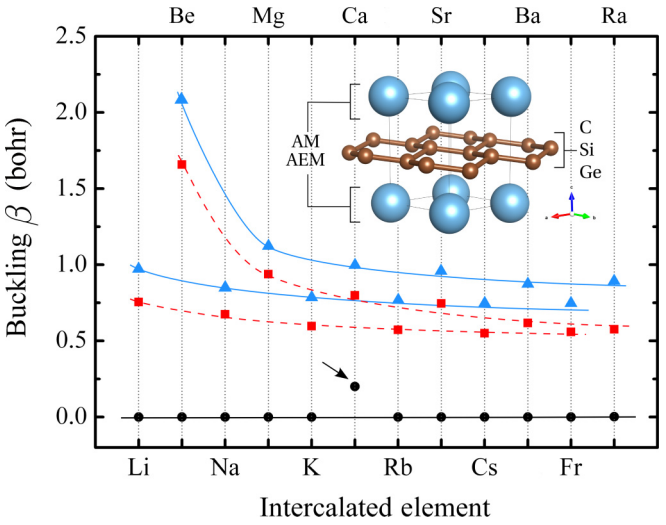

FIG. 1. (Color online) Buckling (β) of the honeycomb layer as a function of the chemical composition from theoretical structural relaxation. Intercalated graphites are shown as black dots, silicides as red squares, and germanides as blue triangles. Lines are guides to the eye to stress the different behaviors of alkali and alkaline-earth intercalations. The inset shows a prototype crystal structure in a buckled configuration ($\beta \neq 0$, $EuGe_2$ crystal type).

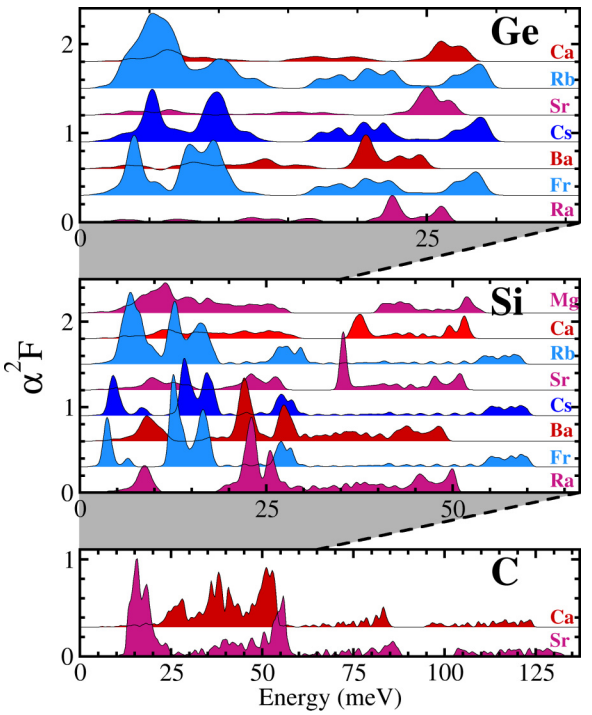

FIG. 2. (Color online) Eliashberg spectral function $\alpha^2F(\omega)$ calculated for dynamically stable materials on the MX_2 set under investigation. These spectral functions show an overall similar behavior, having a low-energy region dominated by intercalant phonon modes, a middle energy range with out-of-plane X-phonon modes, and an high-energy spectra of X-bond stretching modes. These features are also seen in CaC_6 and doped graphene [13,25]. Note that the plots have different frequency scales as the mass of the honeycomb atoms scales the entire spectral function and for both low- and high-energy regions.

Eliashberg spectral functions [33,34] $\alpha^2F(\omega)$ for all the dynamically stable systems are reported in Fig. 2. From now on we will only consider this subset of materials. In this figure we can clearly observe that the spectral functions are scaled in their frequency by the mass of the atom forming the honeycomb layer. And this extends not only, obviously, to the high-energy modes that originate from strong in-layer bonds, but also to the low-frequency modes that are dominated by the intercalant motion in the weak interlayer potential, thus, indicating a chemical effect. We also observe that alkali metals (as compared with alkaline earths) lead to systematically lower phonon branches therefore to enhanced coupling strengths [33],

$$\lambda = 2\int \frac{\alpha^2F(\omega)}{\omega}d\omega, \tag{1}$$

at the same time this lowers the average frequency, that we conventionally express as

$$\omega_{\log} = \exp\left[\frac{2}{\lambda}\int \alpha^2F(\omega)\frac{\ln(\omega)}{\omega}d\omega\right]. \tag{2}$$

From an electronic point of view, all the materials share a qualitatively similar structure. As in the case of CaC_6 or doped graphene, there are two types of electronic states located at the Fermi energy: antibonding π states provided by the honeycomb layer (C, Si, and Ge) and 2D interlayer states with contributions from the M d orbitals. These electronic states hybridize differently along the alkali or the alkaline-earth column and lead to different effective dopings and band alignments. This affects the density of states at the Fermi energy [$N(E_F)$] and with it the occurrence of superconductivity as we will show below.

In order to perform a fast screen of our MX_2 set, the superconducting critical temperatures were estimated within the McMillan-Allen-Dynes parametrization of the Eliashberg equations [33,35–37],

$$T_c = \frac{\omega_{\log}}{1.2k_B}\exp\left[-\frac{1.04(1+\lambda)}{\lambda-\mu^*(1+0.62\lambda)}\right], \tag{3}$$

where k_B is the Boltzmann constant. This formula depends on three parameters: the Coulomb pseudopotential μ^* [here fixed to 0.1 by comparison with density-functional theory for superconductor (SCDFT) results, see below], the logarithmic average of the phonon frequency $\omega_{\log}$, and the coupling constant λ. The computed T_C couplings λ and $\omega_{\log}$ are shown in Fig. 3.

In the limit of a homogeneous coupling in **k** space, λ is proportional to $N(E_F)$. Within BCS theory, this parameter splits as $\lambda = VN(E_F)$, where V is the BCS coupling strength. In Fig. 3(b) we observe a remarkable proportionality between λ and $N(E_F)$, leading to the conclusion that V is approximately the same on this MX_2 class of systems with the sole exception of few systems characterized by strong softening. Eventually this softening will lead to a phononic instability and to a structural phase transition, perhaps under different thermodynamic conditions of pressure and temperature. Although not belonging to this MX_2 family, we observe that CaC_6 lies perfectly in this regime [28,38], and similarly does MgB_2,

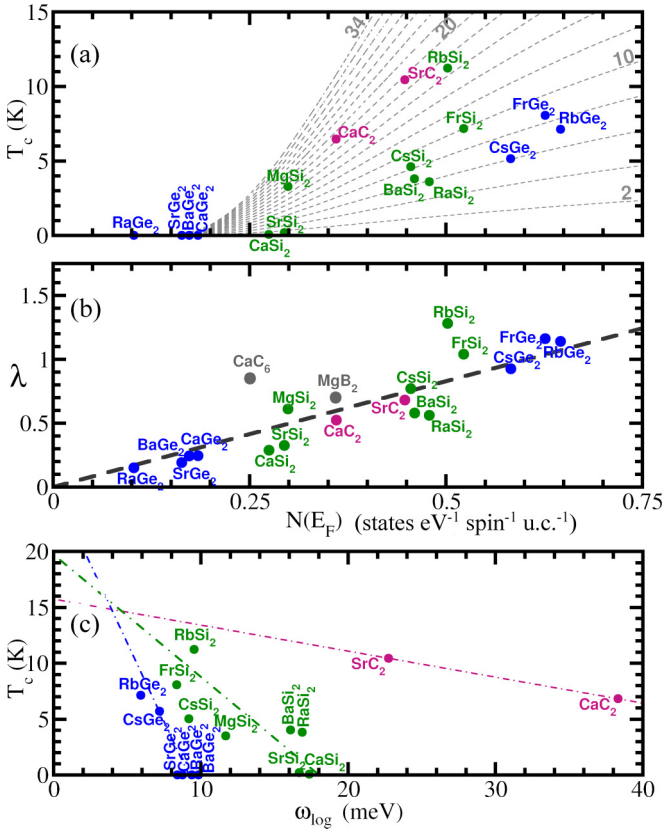

FIG. 3. (Color online) (a) Critical temperatures calculated within the McMillan-Allen Dynes formula [35,36] using $\mu^* = 0.1$. Gray dashed lines are isomass lines representing the phonon energy average $\omega_{\log}$ [Eq. (2)] ranging from 2 to 34 meV; (b) Electron-phonon coupling parameter λ [Eq. (1)] as a function of the density of states at the Fermi level [$N(E_F)$] and per unit cell (u.c.); (c) Critical temperature versus $\omega_{\log}$ (lines serves only as guides to the eye).

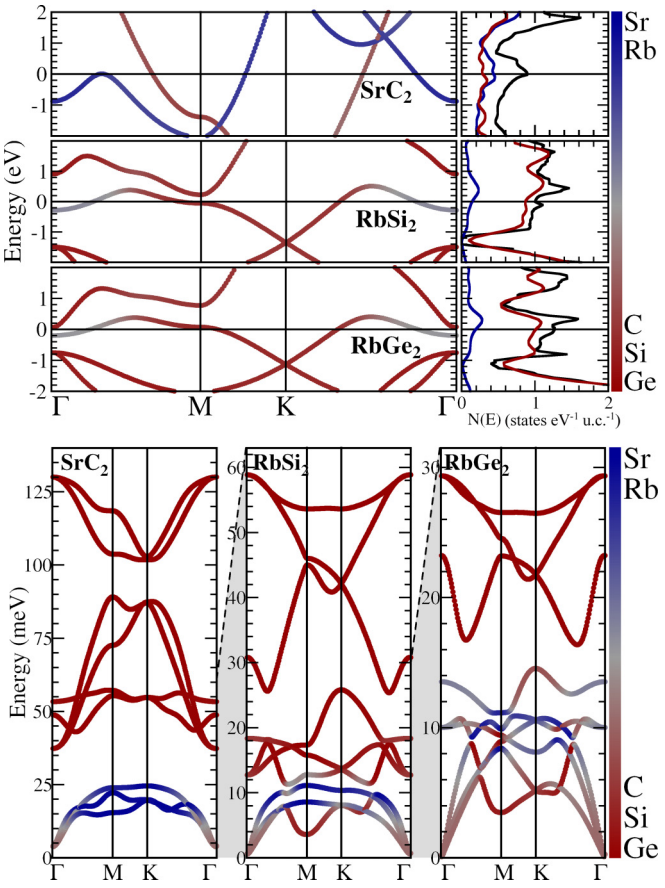

FIG. 4. (Color online) Top: electronic bands in SrC_2, $RbSi_2$, and $RbGe_2$ around the Fermi level (at zero eV). The color scale indicates the projection of the Kohn-Sham states on the atomic orbitals of the intercalating atom. Bottom: phonon dispersion relation. The color scale indicates the component of the phonon mode on the intercalant atom.

however, this is accidental as we have ignored its multiband nature [39–41].

These calculations predict several interesting superconductors and in particular $RbSi_2$, $RbGe_2$, and SrC_2. $RbGe_2$ has the highest density of states and, as discussed above, also presents the highest λ, even though it shows a modest T_C of 7 K. In fact T_C [see Eq. (3)] depends also on the phonon energy, which is larger for systems having lower mass, for instance, SrC_2. Also in this Fig. 3 [in panel (a)], we included the isomass lines as a reference to indicate how the T_C in a material would be affected by λ (on X_2) or by $N(E_F)$. The outcome of this analysis suggests the existence of an upper critical temperature for each family. And this is imposed by the electronic structure as $N(E_F)$ hardly would exceed the value of 0.7 states eV^{-1} $spin^{-1}$ (of $RbGe_2$). Following the isomass lines in this figure for each subfamily leads to the conclusion that upper critical temperatures of about 10, 15, and 20 K, respectively, exist for intercalations in Ge, Si, and carbon honeycombs. We firmly believe that this conclusion can be extended beyond the MX_2 class since different intercalation densities will not plausibly affect the coupling strength. However, the coupling strength could be significantly affected if σ states were involved (as in MgB_2), but this would require an unphysical doping level.

We will now focus our investigation on three selected systems SrC_2, $RbSi_2$, and $RbGe_2$ as the most interesting representative of each subfamily. As discussed in the Introduction both $RbSi_2$ and $RbGe_2$ are stable towards elemental decomposition. In addition they are more stable than their $RbSi_6$ and $RbGe_6$ rhombohedral counterparts [30]. Therefore, we believe, these two systems are likely to be accessible to the experimental synthesis. On the other hand, SrC_2 is not stable with respect to elemental decomposition and turns out to be less energetically competitive than its rhombohedral SrC_6 configuration that, in fact, has been synthesized [42]. Nevertheless, since the system is dynamically stable, it may still be possible to find a way to its synthesis, perhaps by means of a nonequilibrium process or by high temperature and high pressure, as often used to synthesize clathrates [43], carbon borides [44], layered disilicides [15,17,21,22], and germanides [18].

The electronic band structures of these three selected materials are shown in Fig. 4. The bands of SrC_2 essentially differ from those of $RbSi_2$ and $RbGe_2$due to the effect of symmetry breaking (both have buckling) as well as the doping level of the honeycomb lattice (charge projection shows that divalent strontium donates 1.2 electrons—whereas

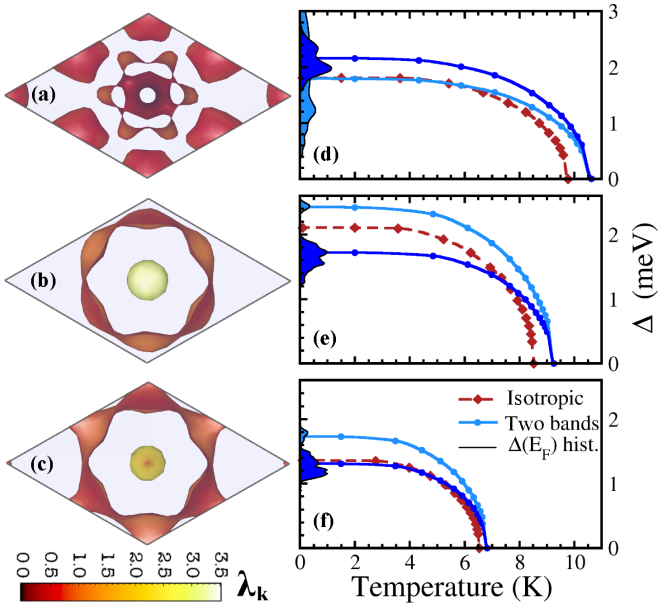

FIG. 5. (Color online) Fermi surface of (a) SrC_2, (b) $RbSi_2$, and (c) $RbGe_2$, shown in the Γ-centered reciprocal unit cell (top view). The color scale (bottom left corner) gives the **k**-resolved electron-phonon coupling [28] λ_k. The superconducting gap as a function of temperature for (d) SrC_2, (e) $RbSi_2$, and (f) $RbGe_2$, computed within the SCDFT [49]. The red-dashed line is the isotropic behavior, and the blue-continuous lines are a minimal two-band approximation. The full gap distribution function [28,38] is given at $T = 0$ as a filled area.

monovalent Rb donates 0.5 electrons for both $RbSi_2$ and $RbGe_2$). The Fermi surfaces (FSs), shown in Figs. 5(a)–5(c), present multiple Fermi sheets with different orbital characters. In SrC_2 the inner FS comes from interlayer states, whereas the outer surface is formed by carbon π states. In $RbSi_2$ and $RbGe_2$ the hybridization between interlayer and honeycomb π states is much stronger. The outer FS is mostly due to Si/Ge π states, whereas the inner FS has an interlayer character, however with a relatively large overlap (25%) to Si/Ge π states.

The phonon dispersion for the three systems is shown in Fig. 4. The overall structure of the phonon modes is the same for the three systems. Low-frequency modes present a strong intercalant component, fundamentally due to the weak force constants that bind the M atoms to their positions in the lattice, but also because of their relatively large masses. For the scope of this paper, the most interesting feature of the phononic dispersion is the behavior of the buckling modes. In the unbuckled (flat) SrC_2 compound this mode has 50 meV in the zone center and cannot fall below 40 meV, whereas in the buckled $RbSi_2$ and $RbGe_2$ compounds it becomes "soft" moving from Γ (at 30 meV in $RbSi_2$ and 23 meV in $RbGe_2$) to M (3.5 meV). This mode is strongly coupled in both $RbSi_2$ and $RbGe_2$, and anharmonic effects (not considered in the present paper) may also affect the strength of its coupling.

We will now reconsider the superconducting properties of these selected systems by means of a more accurate superconductivity theory than the McMillan formula used so far. We will adopt SCDFT as it is completely parameter free [45–47] and allows for a full **k**-resolved description [48].

It should be observed [see Fig. 5, panels (a)–(c)] that the electron-phonon coupling in all these systems is rather anisotropic, meaning strongly **k** dependent on the FS. SrC_2 has a continuous distribution, whereas the two FSs of $RbSi_2$ and $RbGe_2$have remarkably different coupling strengths: stronger on the small FS around the Γ point and weaker on the outer FS (at large $|\mathbf{k}|$). The distribution of superconducting gaps on the Fermi energy (not shown) follows the anisotropy in $\lambda_{\mathbf{k}}$, similar to the behavior observed in bulk lead [50]. The gap distribution function at $T = 0$ (i.e., the energy distribution of the SC gaps: Δ_{k_F}) as well as the temperature dependence (in a two-band and single-band model) are plotted in Figs. 5(d)–5(f). Both $RbSi_2$ and $RbGe_2$ show two distinct gaps (such as in MgB_2 or bulk lead [40,41,50]), whereas SrC_2 has an anisotropic gap continuously distributed. This gap distribution reminds one of CaC_6 [28,51,52]. This anisotropy will affect the specific heat and the thermodynamical properties. However, unlike in MgB_2, the critical temperature is not much affected by it (less than 1 K). The role of coupling anisotropy on the superconducting behavior can be clearly understood within the qualitative model of Suhl *et al.* [53]. The observed combination of a large anisotropy in the gap with a small enhancement in T_C is a consequence of the strong interband coupling between the π states (having a smaller gap) and the interlayer states (that dominate on the larger gap). The gap distribution of SrC_2 is even broader and clearly cannot be completely captured within a two-band model. The system is in fact almost gapless since the small $|\mathbf{k}|$ part of the FS shows a negligible superconducting pairing as a consequence of the weak phononic coupling.

To summarize, we presented a theoretical study on honeycomb-layered binary carbides, silicides, and germanides intercalated by alkali or alkaline-earth metals. Our superconductivity analysis has shown that in this class of materials are many compounds with a relatively high critical temperature (∼10 K) as well as a quite complex superconducting state. In addition, the stability investigation has shown that several compounds should be accessible to their experimental synthesis. Finally, we demonstrate an intrinsic physical similarity among the group, which can be traced back to their characteristic π + interlayer character of states at the Fermi surface. From this feature we estimate an upper limit for the transition critical temperatures: ∼20, ∼15, and ∼10 K, respectively, for carbon, silicon, and germanium intercalated honeycombs. This limit could be broken only in the unlikely case in which the doping level would be able to drive σ states at the Fermi level. Nevertheless this study indicates that superconductivity in doped graphite and similar systems is a rather general behavior, and many more superconductors may still be discovered.

J.A.F.-L. acknowledges financial support from the EU's 7th Framework Marie-Curie scholarship Program within the "ExMaMa" Project (Project No. 329386).

[1] A. K. Geim and K. S. Novoselov, Nature Mater. **6**, 183 (2007).
[2] A. K. Geim, Science **324**, 1530 (2009).
[3] K. S. Novoselov, V. I. Fal'ko, L. Colombo, P. R. Gellert, M. G. Schwab, and K. Kim, Nature (London) **490**, 192 (2012).

[4] K. S. Novoselov, A. K. Geim, S. V. Morozov, D. Jiang, Y. Zhang, S. V. Dubonos, I. V. Grigorieva, and A. A. Firsov, Science **306**, 666 (2004).

[5] A. V. Fedorov, N. I. Verbitskiy, D. Haberer, C. Struzzi, L. Petaccia, D. Usachov, O. Y. Vilkov, D. V. Vyalikh, J. Fink, M. Knupfer, B. Büchner, and A. Grüneis, Nat. Commun. **5**, 3257 (2014).

[6] S.-L. Yang, J. A. Sobota, C. A. Howard, C. J. Pickard, M. Hashimoto, D. H. Lu, S.-K. Mo, P. S. Kirchmann, and Z.-X. Shen, Nat. Commun. **5**, 3493 (2014).

[7] R. A. Klemm, *Layered Superconductors* (Oxford University Press, New York, 2012), Vol. 1.

[8] I. Belash, A. Bronnikov, O. Zharikov, and A. Pal'nichenko, Solid State Commun. **69**, 921 (1989).

[9] V. A. Nalimova, D. Guerard, M. Lelaurain, and O. V. Fateev, Carbon **33**, 177 (1995).

[10] V. V. Avdeeva, V. A. Nalimovaa, and K. N. Semenenko, High Pressure Res. **6**, 11 (1990).

[11] T. E. Weller, M. Ellerby, S. S. Saxena, R. P. Smith, and N. T. Skipper, Nat. Phys. **1**, 39 (2005).

[12] N. Emery, C. Hérold, M. d'Astuto, V. Garcia, C. Bellin, J. F. Marêché, P. Lagrange, and G. Loupias, Phys. Rev. Lett. **95**, 087003 (2005).

[13] G. Profeta, M. Calandra, and F. Mauri, Nat. Phys. **8**, 131 (2012).

[14] S. Sanfilippo, H. Elsinger, M. Nunez-Regueiro, O. Laborde, S. LeFloch, M. Affronte, G. L. Olcese, and A. Palenzona, Phys. Rev. B **61**, R3800 (2000).

[15] P. Bordet, M. Affronte, S. Sanfilippo, M. Nunez-Regueiro, O. Laborde, G. L. Olcese, A. Palenzona, S. LeFloch, D. Levi, and M. Hanfland, Phys. Rev. B **62**, 11392 (2000).

[16] M. Imai, T. Hirano, T. Kikegawa, and O. Shimomura, Phys. Rev. B **58**, 11922 (1998).

[17] M. Imai and T. Kikegawa, Chem. Mater. **15**, 2543 (2003).

[18] P. H. Tobash and S. Bobev, J. Solid State Chem. **180**, 1575 (2007).

[19] S. Bobev, E. D. Bauer, J. D. Thompson, J. L. Sarrao, G. J. Miller, B. Eck, and R. Dronskowski, J. Solid State Chem. **177**, 3545 (2004).

[20] M. Imai, K. Hirata, and T. Hirano, Physica C **245**, 12 (1995).

[21] J. A. Flores-Livas, R. Debord, S. Botti, A. San Miguel, M. A. L. Marques, and S. Pailhès, Phys. Rev. Lett. **106**, 087002 (2011).

[22] J. Evers and A. Weiss, Mater. Res. Bull. **9**, 549 (1974).

[23] R. Demchyna, S. Leoni, H. Rosner, and U. Schwarz, Z. Kristallogr. **221**, 420 (2006).

[24] S. Yamanaka, Dalton Trans. **39**, 1901 (2009).

[25] M. Calandra and F. Mauri, Phys. Rev. Lett. **95**, 237002 (2005).

[26] L. Boeri, G. B. Bachelet, M. Giantomassi, and O. K. Andersen, Phys. Rev. B **76**, 064510 (2007).

[27] J. S. Kim, L. Boeri, R. K. Kremer, and F. S. Razavi, Phys. Rev. B **74**, 214513 (2006).

[28] A. Sanna, G. Profeta, A. Floris, A. Marini, E. K. U. Gross, and S. Massidda, Phys. Rev. B **75**, 020511 (2007).

[29] We used the two plane-wave-based codes ABINIT [54] and ESPRESSO [55] within the Perdew-Burke-Ernzerhof [56] exchange-correlation functional, and the core states were accounted for by norm-conserving Troullier-Martins pseudopotentials [57]. The pseudopotential accuracy has been checked against the all-electron (LAPW + lo) method as implemented in the ELK code [http://elk.sourceforge.net/].

[30] See Supplemental Material at http://link.aps.org/supplemental/10.1103/PhysRevB.91.054508 for the calculation of the thermodynamic stability of the compounds used in this paper.

[31] Y.-L. Li, W. Luo, Z. Zeng, H.-Q. Lin, H.-k. Mao, and R. Ahuja, Proc. Natl. Acad. Sci. U.S.A. **110**, 9289 (2013).

[32] The phonon spectrum and the electron-phonon matrix elements were obtained employing density-functional perturbation theory [58–60] within the pseudopotential approximation. A cutoff energy of 60 Ry was used in the plane-wave expansion. A $16 \times 16 \times 12$ Monkhorst-Pack k grid and a $4 \times 4 \times 2q$ grid were used for all the materials under consideration with the only exception of SrC_2, $RbSi_2$, and $RbGe_2$ where we have increased the q-sampling grid to $8 \times 8 \times 6$ in order to achieve an accurate description of anisotropic properties.

[33] J. P. Carbotte, Rev. Mod. Phys. **62**, 1027 (1990).

[34] P. B. Allen and B. Mitrović, in *Solid State Physics*, edited by F. Seitz, D. Turnbull, and H. Ehrenreich (Academic, New York, 1982), pp. 1–92.

[35] W. L. McMillan, Phys. Rev. **167**, 331 (1968).

[36] P. B. Allen and R. C. Dynes, Phys. Rev. B **12**, 905 (1975).

[37] G. M. Eliashberg, Zh. Eksp. Teor. Fiz. **38**, 966 (1960) [Sov. Phys. JETP **11**, 696 (1960)].

[38] A. Sanna, S. Pittalis, J. K. Dewhurst, M. Monni, S. Sharma, G. Ummarino, S. Massidda, and E. K. U. Gross, Phys. Rev. B **85**, 184514 (2012).

[39] A. Y. Liu, I. I. Mazin, and J. Kortus, Phys. Rev. Lett. **87**, 087005 (2001).

[40] A. Floris, G. Profeta, N. N. Lathiotakis, M. Lüders, M. A. L. Marques, C. Franchini, E. K. U. Gross, A. Continenza, and S. Massidda, Phys. Rev. Lett. **94**, 037004 (2005).

[41] A. Floris, A. Sanna, M. Lüders, G. Profeta, N. Lathiotakis, M. Marques, C. Franchini, E. Gross, A. Continenza, and S. Massidda, Physica C **456**, 45 (2007).

[42] J. S. Kim, L. Boeri, J. R. O'Brien, F. S. Razavi, and R. K. Kremer, Phys. Rev. Lett. **99**, 027001 (2007).

[43] P. Toulemonde, C. Adessi, X. Blase, A. San Miguel, and J. L. Tholence, Phys. Rev. B **71**, 094504 (2005).

[44] S. Shah and A. N. Kolmogorov, Phys. Rev. B **88**, 014107 (2013).

[45] L. N. Oliveira, E. K. U. Gross, and W. Kohn, Phys. Rev. Lett. **60**, 2430 (1988).

[46] M. Lüders, M. A. L. Marques, N. N. Lathiotakis, A. Floris, G. Profeta, L. Fast, A. Continenza, S. Massidda, and E. K. U. Gross, Phys. Rev. B **72**, 024545 (2005).

[47] M. A. L. Marques, M. Lüders, N. N. Lathiotakis, G. Profeta, A. Floris, L. Fast, A. Continenza, E. K. U. Gross, and S. Massidda, Phys. Rev. B **72**, 024546 (2005).

[48] The phononic functional we use is an improved version with respect to Refs. [46,47] and is discussed in Ref. [49]. Coulomb interactions are included within static random-phase approximation [28].

[49] A. Sanna and E. K. U. Gross, Density functional theory for superconductors: Migdal functional from the Sham-Schlueter connection (unpublished).

[50] A. Floris, A. Sanna, S. Massidda, and E. K. U. Gross, Phys. Rev. B **75**, 054508 (2007).

[51] R. S. Gonnelli, D. Daghero, D. Delaude, M. Tortello, G. A. Ummarino, V. A. Stepanov, J. S. Kim, R. K. Kremer, A. Sanna, G. Profeta, and S. Massidda, Phys. Rev. Lett. **100**, 207004 (2008).

[52] U. Nagel, D. Hüvonen, E. Joon, J. S. Kim, R. K. Kremer, and T. Rõom, Phys. Rev. B **78**, 041404 (2008).
[53] H. Suhl, B. Matthias, and L. Walker, Phys. Rev. Lett. **3**, 552 (1959).
[54] X. Gonze *et al.*, Comput. Phys. Commun. **180**, 2582 (2009).
[55] P. Giannozzi *et al.*, J. Phys.: Condens. Matter **21**, 395502 (2009).
[56] J. P. Perdew, K. Burke, and M. Ernzerhof, Phys. Rev. Lett. **77**, 3865 (1996).
[57] M. Fuchs and M. Scheffler, Comput. Phys. Commun. **119**, 67 (1999).
[58] S. Baroni, S. de Gironcoli, A. Dal Corso, and P. Giannozzi, Rev. Mod. Phys. **73**, 515 (2001).
[59] X. Gonze and J.-P. Vigneron, Phys. Rev. B **39**, 13120 (1989).
[60] S. Y. Savrasov and D. Y. Savrasov, Phys. Rev. B **54**, 16487 (1996).